BRAIN SURFACE CONFORMAL PARAMETERIZATION

Yalin Wang
Mathematics Department, UCLA
email: ylwang@math.ucla.edu

Xianfeng Gu
Computer Science Department
SUNY at Stony Brook
emai: gu@cs.sunysb.edu

Kiralee M. Hayashi
Laboratory of Neuro Imaging
UCLA School of Medicine
email: khayashi@loni.ucla.edu

Tony F. Chan
Mathematics Department, UCLA
email: chan@math.ucla.edu

Paul M. Thompson
Laboratory of Neuro Imaging
UCLA School of Medicine
email: thompson@loni.ucla.edu

Shing-Tung Yau
Department of Mathematics
Harvard University
email: yau@math.harvard.edu

ABSTRACT
We develop a general approach that uses holomorphic 1-forms to parameterize anatomical surfaces with complex (possibly branching) topology. Rather than evolve the surface geometry to a plane or sphere, we instead use the fact that all orientable surfaces are Riemann surfaces and admit conformal structures, which induce special curvilinear coordinate systems on the surfaces. We can then automatically partition the surface using a critical graph that connects zero points in the conformal structure on the surface. The trajectories of iso-parametric curves canonically partition a surface into patches. Each of these patches is either a topological disk or a cylinder and can be conformally mapped to a parallelogram by integrating a holomorphic 1-form defined on the surface. The resulting surface subdivision and the parameterizations of the components are intrinsic and stable. To illustrate the technique, we computed conformal structures for several types of anatomical surfaces in MRI scans of the brain, including the cortex, hippocampus, and lateral ventricles. We found that the resulting parameterizations were consistent across subjects, even for branching structures such as the ventricles, which are otherwise difficult to parameterize. Compared with other variational approaches based on surface inflation, our technique works on surfaces with arbitrary complexity while guaranteeing minimal distortion in the parameterization. It also generates grids on surfaces for PDE-based signal processing.

KEY WORDS
Brain Mapping, Riemann Surface Structure, Conforaml Net, Critical Graph

1 Introduction

Surface-based modeling is valuable in brain imaging to help analyze anatomical shape, to statistically combine or compare 3D anatomical models across subjects, and to map functional imaging parameters onto anatomical surfaces. Multiple surfaces can be registered nonlinearly to construct a mean shape for a group of subjects, and deformation mappings can encode shape variations around the mean. This type of deformable surface registration has been used to detect developmental and disease effects on brain structures such as the corpus callosum and basal ganglia [1], the hippocampus [2], and the cortex [3]. Nonlinear matching of brain surfaces can also be used to track the progression of neurodegenerative disorders such as Alzheimer's disease [2], to measure brain growth in development [1], and to reveal directional biases in gyral pattern variability [4].

Parameterization of anatomical surface models involves computing a smooth (differentiable) one-to-one mapping of regular 2D coordinate grids onto the 3D surfaces, so that numerical quantities can be computed easily from the resulting models. Even so, it is often difficult to smoothly deform a complex 3D surface to a sphere or 2D plane without substantial angular or area distortion. Here we present a new method to parameterize brain surfaces based on their Riemann surface structure. By contrast with variational approaches based on surface inflation, our method can parameterize surfaces with arbitrary complexity including branching surfaces not topologically homeomorphic to a sphere (higher-genus objects) while formally guaranteeing minimal distortion.

1.1 Previous Work

Brain surface parameterization has been studied intensively. Schwartz et al. [5], and Timsari and Leahy [6] computed quasi-isometric flat maps of the cerebral cortex. Hurdal and Stephenson [7] report a discrete mapping approach that uses circle packings to produce "flattened" images of cortical surfaces on the sphere, the Euclidean plane, and the hyperbolic plane. The obtained maps are quasi-conformal approximations of classical conformal maps. Haker et al. [8] implemented a finite element approximation for parameterizing brain surfaces via conformal mappings. They selected a point on the cortex to map to the north pole and conformally mapped the rest of the cortical surface to the complex plane by stereographic projection of the Riemann sphere to the complex plane. Gu et al. [9] proposed a method to find a unique conformal mapping between any two genus zero manifolds by minimizing the harmonic energy of the map. They demonstrated this

method by conformally mapping the cortical surface to a sphere.

In computational anatomy, 3D shape analyses are often performed to analyze the geometry of specific brain structures, and compute statistical information on anatomical variability and group differences. Joshi et al. [10] analyzed the shape of the hippocampus via a spatially normalizing elastic transformation. Group differences in surface shape were identified by comparing the transformations required to map individual surfaces to a group average surface [2]. Kelemen et al. [11] studied 3D hippocampal shapes based on a boundary description using spherical harmonic basis functions (SPHARM). The SPHARM shape description creates an implicit boundary correspondence between shapes. Later, Gerig et al. [12] used SPHARM to study ventricular size and shape in 3D MRI scans of monozygotic and dizygotic twin pairs. Pizer et al. [13] proposed a method to apply sampled medial models (M-reps) to shape analysis. By holding the topology of the model fixed, an implicit correspondence between surface boundary points and an underlying medial curve is established and can be applied to model anatomy in radiation oncology and for shape analysis.

1.2 Theoretical Background and Definitions

A *manifold* of dimension n is a connected Hausdorff space M for which every point has a neighborhood U that is homeomorphic to an open subset V of R^n. Such a homeomorphism $\phi : U \to V$ is called a coordinate chart. An *atlas* is a family of charts $\{U_\alpha, \phi_\alpha\}$ for which U_α constitute an open covering of M.

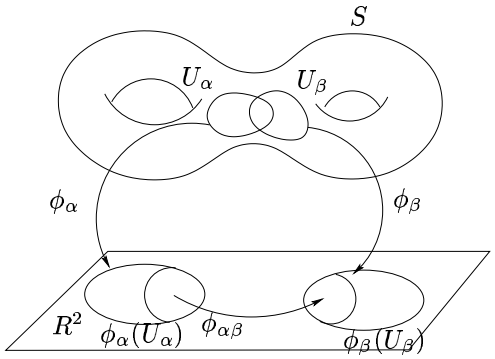

Figure 1. The Structure of a Manifold. An atlas is a family of charts that jointly form an open covering of the manifold.

Suppose $\{U_\alpha, \phi_\alpha\}$ and $\{U_\beta, \phi_\beta\}$ are two charts on a manifold S, $U_\alpha \cap U_\beta \neq \Phi$, then the chart transition is defined as $\phi_{\alpha\beta} : \phi_\alpha(U_\alpha \cap U_\beta) \to \phi_\beta(U_\alpha \cap U_\beta)$. An atlas $\{U_\alpha, \phi_\alpha\}$ on a manifold is called *differentiable* if all chart transitions are differentiable of class C^∞. A chart is called *compatible* with a differentiable atlas if adding this chart to the atlas still yields a differentiable atlas. The set of all charts compatible with a given differentiable atlas yields a *differentiable structure*. A *differentiable manifold* of dimension n is a manifold of dimension n together with a differentiable structure.

For a manifold M with an atlas $\mathcal{A} = \{U_\alpha, \phi_\alpha\}$, if all chart transition functions

$$\phi_{\alpha\beta} = \phi_\beta \circ \phi_\alpha^{-1} : \phi_\alpha(U_\alpha \cap U_\beta) \to \phi_\beta(U_\alpha \cap U_\beta)$$

are holomorphic, then $\mathcal{A}$ is a conformal atlas for M. A chart $\{U_\alpha, \phi_\alpha\}$ is *compatible* with an atlas $\mathcal{A}$, if the union $\mathcal{A} \cup \{U_\alpha, \phi_\alpha\}$ is still a conformal atlas.

Two conformal atlases are compatible if their union is still a conformal atlas. Each conformal compatible equivalence class is a conformal structure. A 2-manifold with a conformal structure is called a *Riemann surface*. It has been proven that all metric orientable surfaces are Riemann surfaces.

Holomorphic and meromorphic functions and differential forms can be generalized to Riemann surfaces by using the notion of conformal structure. For example, a *holomorphic* one-form ω is a complex differential form, such that in each local frame $z_\alpha = (u_\alpha, v_\alpha)$, the parametric representation is $\omega = f(z_\alpha)dz_\alpha$, where $f(z_\alpha)$ is a holomorphic function. On a different chart $\{U_\beta, \phi_\beta\}$, $\omega = f(z_\alpha(z_\beta))\frac{dz_\alpha}{dz_\beta}dz_\beta$. For a genus g closed surface, all holomorphic one-forms form a real $2g$ dimensional linear space.

At a *zero point* $p \in M$ of a holomorphic one-form ω, any local parametric representation $\omega = f(z_\alpha)dz_\alpha, f|_p = 0$. According to the Riemann-Roch theorem, in general there are $2g - 2$ zero points for a holomorphic one-form defined on a surface of genus g.

A holomorphic one-form induces a special system of curves on a surface, the so-called *conformal net*. A curve $\gamma \subset M$ is called a horizontal trajectory of ω, if $\omega^2(d\gamma) \geq 0$; similarly, γ is a vertical trajectory if $\omega^2(d\gamma) < 0$. The horizontal and vertical trajectories form a web on the surface. The trajectories that connect zero points, or a zero point with the boundary are called *critical trajectories*. The critical horizontal trajectories form a graph, which is called the *critical graph*. In general, the behavior of a trajectory may be very complicated, it may have infinite length and may be dense on the surface. If the critical graph is finite, then all the horizontal trajectories are finite. The critical graph partitions the surface into a set of non-overlapping patches that jointly cover the surface, and each patch is either a topological disk or a topological cylinder. Each patch $\Omega \subset M$ can be mapped to the complex plane using the following formulae. Suppose we pick a base point $p_0 \in \Omega$, and any path γ that connects p_0 to p. Then if we define $\phi(p) = \int_\gamma \omega$, the map ϕ is conformal, and $\phi(\Omega)$ is a parallelogram. We say ϕ is the conformal parameterization of M induced by ω. ϕ maps the vertical and the horizontal trajectories to iso-u and iso-v curves respectively on the parameter plane. The structure of the critical graph and the parameterizations of the patches are determined by the conformal structure of the surface. If two surfaces share similar

topologies and geometries, they can support consistent critical graphs and segmentations (i.e. surface partitions), and the parameterizations are consistent as well. Therefore, by matching their parameter domains, the entire surfaces can be directly matched in 3D. This generalizes prior work in medical imaging that has matched surfaces by computing a smooth bijection to a single canonical surface, such as a sphere or disk.

A Riemannian metric is a differential quadratic form on a differential manifold. On each chart $\{U_\alpha, \phi_\alpha\}$, it can be represented as

$$ds^2 = E(u,v)du^2 + 2F(u,v)dudv + G(u,v)dv^2.$$

A special conformal structure can be chosen, such that the local parametric representation of Riemannian metric is $ds^2 = \lambda(u,v)(du^2 + dv^2)$. In this case, the local coordinates of each chart are also called *isothermal coordinates*, and $\lambda(u,v)$ is called the *conformal factor*.

This paper takes the advantage of conformal structures of surfaces, consistently segments them and parameterizes the patches using a holomorphic 1-form.

We call the process of finding critical graph and segmentation as the *holomorphic flow segmentation*, which is completely determined by the geometry of the surface and the choice of the holomorphic 1-form. (Note that this differs from the typical meaning of segmentation in medical imaging, and is concerned with the segmentation, or partitioning, of a general surface). Computing holomorphic 1-forms is equivalent to solving elliptic differential equations on the surfaces, and in general, elliptic differential operators are stable. Therefore the resulting surface segmentations and parameterizations are intrinsic and stable, and are applicable for matching noisy surfaces derived from medical images.

2 Holomorphic Flow Segmentation

To compute the holomorphic flow segmentation of a surface, first we compute the conformal structure of the surface; then we select one holomorphic differential form, and locate the zero points on it. By tracing horizontal trajectories through the zero points, the critical graph can be constructed and the surface is divided into several patches. Each patch can then be conformally mapped to a planar parallelogram by integrating the holomorphic differential form.

In our work, surfaces are represented as triangular meshes, namely piecewise polygonal surfaces.The computations with differential forms are based on solving elliptic partial differential equations on surfaces using the finite element method.

2.1 Computing Conformal Structures

A method for computing the conformal structure of a surface was introduced in [14]. Suppose M is a closed genus $g > 0$ surface with a conformal atlas $\mathcal{A}$. The conformal structure $\mathcal{A}$ induces holomorphic 1-forms; all holomorphic 1-forms form a linear space $\Omega(M)$ of dimension $2g$ which is isomorphic to the first cohomology group of the surface $H^1(M, \mathcal{R})$. The set of holomorphic one-forms determines the conformal structure. Therefore, computing conformal structure of M is equivalent to finding a basis for $\Omega(M)$.

The holomorphic 1-form basis $\{\omega_i, i = 1, 2, \cdots, 2g\}$ is computed as follows: compute the homology basis, find the dual cohomology basis, diffuse the cohomology basis to a harmonic 1-form basis, and then convert the harmonic 1-form basis to holomorphic 1-form basis by using the Hodge star operator. The details of the computation are given in [14].

For surfaces with boundaries, we apply the conventional *double covering* technique, which glues two copies of the same surface along their corresponding boundaries to form a symmetric closed surface. Then we apply the above procedure to find the holomorphic 1-form basis.

In terms of data structure, a holomorphic 1-form is represented as a vector-valued function defined on the edges of the mesh $\omega_i : K_1 \to R^2, i = 1, 2 \cdots, 2g,$.

2.2 Selecting the Optimal Holomorphic 1-form

Given a Riemann surface M, there are infinitely many holomorphic 1-forms, but each of them can be expressed as a linear combination of the basis elements. We define a canonical conformal parameterization as any linear combination of the set of holomorphic basis functions ω_i, $i = 1, ..., g$. They satisfy

$$\int_{\zeta_i} \omega_j = \delta_i^j,$$

where $\zeta_i, i = 1, ...n$ are homology bases and δ_i^j is the Kronecker symbol. Then we compute a *canonical conformal parameterization*

$$\omega = \sum_{i=1}^{n} \omega_i.$$

We select a specific parameterization one that maximizes the uniformity of the induced grid over the entire domain using the algorithms introduced in [15], for the purpose of locating zero points in the next step.

2.3 Locating Zero Points

For surface with genus $g > 1$, any holomorphic 1-form ω has $2g - 2$ zero points. The horizontal trajectories through the zero points will partition the surface into several patches. Each patch is either a topological disk or a cylinder, and can be conformally parameterized by ω using $\phi(p) = \int_\gamma \omega$.

Estimating the Conformal Factor Suppose we already have a global conformal parameterization, induced by a holomorphic 1-form ω. Then we can estimate the conformal factor at each vertex, using the following formulae:

$$\lambda(v) = \frac{1}{n} \sum_{[u,v] \in K_1} \frac{|\omega([u,v])|^2}{|r(u) - r(v)|^2}, u, v \in K_0, \quad (1)$$

where n is the valence of vertex v.

Locating Zero Points We find the cluster of vertices with relatively small conformal factors (the lowest $5 - 6\%$). These are candidates for zero points. We cluster all the candidates using the metric on the surface. For each cluster, we pick the vertex that is closest to the center of gravity of the cluster, using the surface metric to define geodesic distances.

Because the triangulation is finite and the computation is an approximation, the number of zero points may not equal the Euler number. In this case, we refine the triangulation of the neighborhood of the zero point candidate and refine the holomorphic 1-form ω.

2.4 Holomorphic Flow Segmentation

Tracing Horizontal Trajectories Once the zero points are located, the horizontal trajectories through them can be traced.

First we choose a neighborhood U_v of a vertex v representing a zero point, U_v is a set of neighboring faces of v, then we map it to the parameter plane by integrating ω. Suppose a vertex $w \in U_v$, and a path composed by a sequence of edges on the mesh is γ, then the parameter location of w is $\phi(w) = \int_\gamma \omega$.

The map $\phi(w)$ is a piecewise linear map. Then the horizontal trajectory is mapped to the horizontal line $y = 0$ in the plane. We slice $\phi(U_v)$ using the line $y = 0$ by edge splitting operations. Suppose the boundary of $\phi(U_v)$ intersects $y = 0$ at a point v', then we choose a neighborhood of v' and repeat the process.

Each time we extend the horizontal trajectory and encounter edges intersecting the trajectory, we insert new vertices at the intersection points, until the trajectory reaches another zero point or the boundary of the mesh. We repeat the tracing process until each zero point connects 4 horizontal trajectories.

Critical Graph Given a surface M and a holomorphic 1-form ω on M, we define the graph $G(M, \omega) = \{V, E, F\}$, as the critical graph of ω. Here V is the set of zero points of ω, E is the set of horizontal trajectories connecting zero points or the boundary segments of M, and F is the set of surface patches segmented by E.

3 Experimental Results

We tested our algorithm on various surfaces, including anatomic surfaces extracted from 3D MRI scans of the brain, and synthetic geometric examples to illustrate the approach. Figure 2 (a)-(d) shows a closed genus 2 surface. We visualized the conformal structure by projecting a checkerboard image back onto the surface (Figure 2 (a)). There is a zero point shown in Figure 2 (a). Another zero point is on the back of the "figure-eight" shaped surface and is symmetric to this zero point. The traced horizontal and vertical trajectories are shown in Figure 2 (c). From the computed conformal structure, the "figure-eight" surface can be segmented into two patches (Figure 2 (c)). Each patch can then be conformally mapped to a rectangle (Figure 2 (d)).

Figure 2 (e)-(g) shows experimental results for a hippocampal surface, a structure in the medial temporal lobe of the brain. The original surface is shown in (e). We leave two holes on the front and back of the hippocampal surface, representing its anterior junction with the amygdala, and its posterior limit as it turns into the white matter of the fornix. It can be logically represented as an open boundary genus one surface, a cylinder (note that spherical harmonic representations would also be possible, if the ends were closed). The computed conformal structure is shown in (f). A horizontal trajectory curve is shown in (g). Cutting the surface along this curve, we can then conformally map the hippocampus to a rectangle. Since the surface of rectangle is similar to the one of hippocampus, the detailed surface information is well preserved in (h). Compared with other spherical parameterization methods, which may have high-valence nodes and dense tiles at the poles of the spherical coordinate system, our parameterization can represent the surface with minimal distortion.

Shape analysis of the lateral ventricles is of great interest in the study of psychiatric illnesses, including schizophrenia, and in degenerative diseases such as Alzheimer's disease. These structures are often enlarged in disease and can provide sensitive measures of disease progression. We can optimize the conformal parameterization by topology modification. For the lateral ventricle surface in each brain hemisphere, we introduce five cuts. Since these cutting positions are at the end of the frontal, occipital, and temporal horns of the ventricles, they can potentially be located automatically. The upper row in Figure 3 shows 5 cuts introduced on two subjects ventricular surfaces. After the cutting, the surfaces become open boundary genus 4 surfaces.

The middle two rows of Figure 3 show parameterizations of the lateral ventricles of the brain. The second row shows the results of parameterizing a ventricular surface for a 65-year-old patient with HIV/AIDS (note the disease-related enlargement)and the third row shows the results for the ventricular model of a 21-year-old control subject. The surfaces are initially generated by using an unsupervised tissue classifier to isolate a binary map of the cerebrospinal

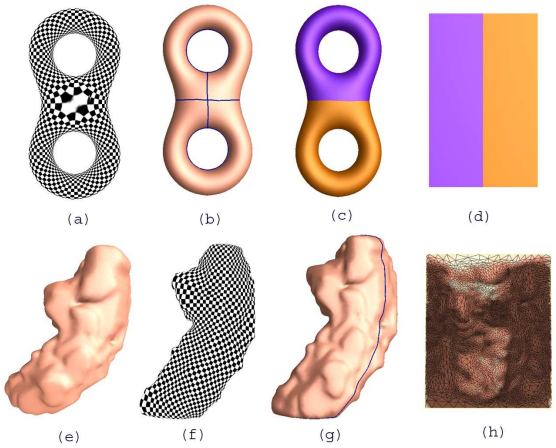

Figure 2. The holomorphic flow segmentation results on a synthetic surface and a hippocampus surface. (a) conformal parameterization of a two hole torus surface. (b) the result of iso-parameter tracing from the detected zero points. (d) the two rectangles to which two segments in (c) are conformally mapped. (f) a conformal parameterization of the hippocampus surface in (e). (g) an iso-parameter curve used to unfold the surface. (h) the rectangle the surface is conformally mapped to.

fluid in the MR image, and tiling the surface of the largest connected component inside the brain. There are a total of 3 zero points on each of the ventricular surfaces. Two of them are located at the middle part of the two "arms" (where the temporal and occipital horns join at the ventricular atrium), as shown by the large black dots in the second row. The third zero point is located in the middle of the model, where the frontal horns are closest to each other. Based on the computed conformal structure, we can partition the surface into 6 patches. Each patch can be conformally mapped to a rectangle. Although the two brain ventricle shapes are very different, the segmentation results are consistent in that the surfaces are partitioned into patches with the same relative arrangement and connectivity.

Finally, the conformal grids induced here are orthogonal and therefore especially suitable for numerical discretization of partial differential equation (PDEs) on brain surfaces. Surface-based PDEs are useful for elastic registration of surfaces, for EEG/MEG reconstruction, for signal denoising and regularization, and for generation of geodesic paths on surfaces. By using global conformal parameterization, these problems can be converted into solving PDEs on planar domains. Using the conformal factor and the Riemannian metric tensor, we can implement covariant differentiation easily. Figure 4 shows illustrative examples of fluid flow simulation by solving the Navier-Stokes equation on the hippocampus surface. Although these are artificial examples, they illustrate the feasibility of discretizing PDEs on the conformal grids developed here. Compared with other work [16], our approach is relatively efficient and avoids some complexity in handling complicated boundary constraints. We are currently extending this work to implement more general differential operators on brain surfaces, for using in nonlinear surface registration and surface-based signal processing.

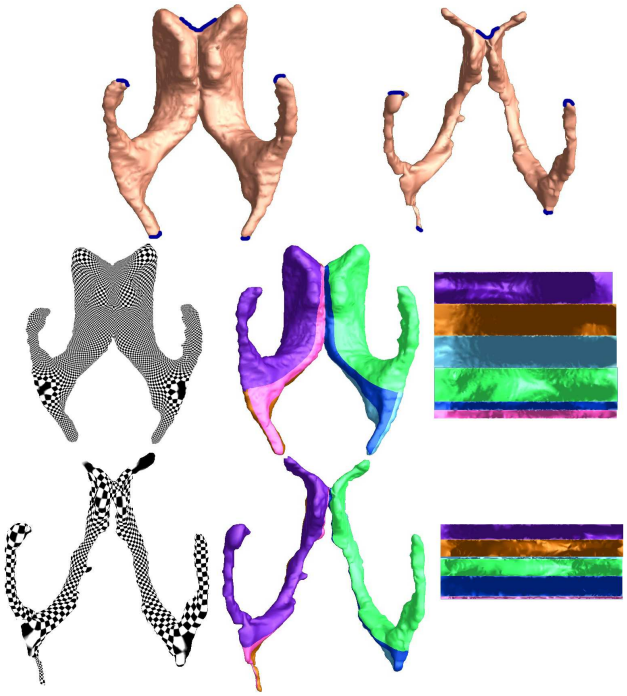

Figure 3. Illustrates surface parameterization results for the lateral ventricles. The upper row shows 5 cuts are introduced and they convert the lateral ventricle surface into a genus 4 surface. The second row shows models parameterized using holomorphic 1-forms, for a 65-year- old subject with HIV/AIDS and the third row shows the same maps computed for a healthy 21-year-old control subject. The computed conformal structure, holomorphic flow segmentation and their associated parameter domains are shown.

4 Conclusion and Future Work

In this paper, we presented a brain surface parameterization method that invokes the Riemann surface structure to generate conformal grids on surfaces of arbitrary complexity (including branching topologies). For high genus surfaces, a global conformal parameterization induces a canonical segmentation, i.e. there is a discrete partition of the surface into conformally parameterized patches. Each partition is either a topological disk or a cylinder and can be conformally mapped to a rectangle in the parameter domain. We demonstrated the parameterization for both closed and open boundary surfaces. We tested our algorithm on the hippocampus and lateral ventricle surfaces. The grid generation algorithm is intrinsic (i.e. does not depend on any initial choice of surface coordinates) and is stable, as shown

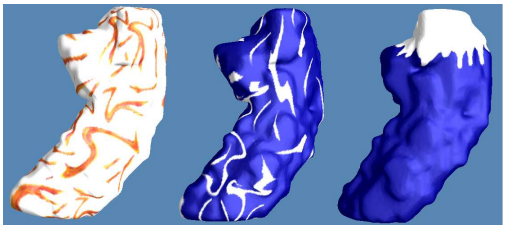

Figure 4. Illustrates solving the Navier-Stokes equation for fluid propagations on brain surfaces. Although these are artificial examples, they show the feasibility of discretizing PDEs on the conformal grid structure, which can ensure numerical accuracy for various applications of PDE-based signal processing on anatomical surfaces.

by grids induced on ventricles of various shapes and sizes. Compared with other work conformally mapping brain surfaces to sphere, our work may introduce less distortion and may be especially convenient for other post-processing work such as surface registration and landmark matching. Our future work will focus on signal processing on brain surfaces, as well as brain surface registration and shape and asymmetry analysis for subcortical structures.

References

[1] P.M. Thompson, J.N. Giedd, R.P. Woods, D. MacDonald, A.C. Evans, and A.W. Toga. Growth patterns in the developing brain detected by using continuum-mechanical tensor maps. *Nature*, 404(6774):190–193, March 2000.

[2] J.G. Csernansky, S. Joshi, L.E. Wang, J. Haller, M. Gado, J.P. Miller, U. Grenander, and M.I. Miller. Hippocampal morphometry in schizophrenia via high dimensional brain mapping. *Proc. Natl. Acad. Sci.*, 95:11406–11411, September 1998.

[3] P.M. Thompson, R.P. Woods, M.S. Mega, and A.W. Toga. Mathematical/computational challenges in creating population-based brain atlases. In *Human Brain Mapping*, volume 9, pages 81–92, Feb. 2000.

[4] G.L. Kindlmann, D.M. Weinstein, A.D. Lee, A.W. Toga, and P.M. Thompson. Visualization of anatomic covariance tensor fields. In *Proc. IEEE Engineering in Medicine and Biology Society (EMBS)*, San Fransisco, CA, Sept. 1-5 2004.

[5] E.L. Schwartz, A. Shaw, and E. Wolfson. A numerical solution to the generalized mapmaker's problem: Flattening nonconvex polyhedral surfaces. *IEEE Transactions on Pattern Analysis and Machine Intelligence*, 11(9):1005–1008, Sep. 1989.

[6] B. Timsari and R. Leahy. An optimization method for creating semi-isometric flat maps of the cerebral cortex. In *Proceedings of SPIE, Medical Imaging*, San Diego, CA, Feb. 2000.

[7] M. K. Hurdal and K. Stephenson. Cortical cartography using the discrete conformal approach of circle packings. *NeuroImage*, 23:S119–S128, 2004.

[8] S. Angenent, S. Haker, A. Tannenbaum, and R. Kikinis. Conformal geometry and brain flattening. *MICCAI*, pages 271–278, 1999.

[9] X. Gu, Y. Wang, T.F. Chan, P.M. Thompson, and S.-T. Yau. Genus zero surface conformal mapping and its application to brain surface mapping. *IEEE Trans. on Med. Imaging*, 23(8):949–958, Aug. 2004.

[10] S. Joshi, M. Miller, and U. Grenander. On the geometry and shape of brain sub-manifolds. *IEEE PAMI*, 11:1317–1343, 1997.

[11] A. Kelemen, G. Székely, and G. Gerig. Elastic model-based segmentation of 3d neuroradiological data sets. *IEEE Trans. Med. Imaging*, 18(10):828–839, Oct. 1999.

[12] G. Gerig, M. Styner, D. Jones, D. Weinberger, and J. Lieberman. Shape analysis of brain ventricles using spharm. In *Proc. MMBIA 2001*, pages 171–178. IEEE Computer Society, Dec. 2001.

[13] S. Pizer, D. Fritsch, P. Yushkevich, V. Johnson, and E. Chaney. Segmentation, registration, and measurement of shape variation via image object shape. *IEEE Trans. Med. Imaging*, 18:851–865, Oct. 1999.

[14] X. Gu and S.T. Yau. Computing conformal structures of surfaces. *Communication of Information and Systems*, December 2002.

[15] M. Jin, Y. Wang, S.T. Yau, and X. Gu. Optimal global conformal surface parameterization for visualization. In *IEEE Visualization*, pages 267–274, Austin, TX, Oct. 2004.

[16] J. Stam. Flows on surfaces of arbitrary topology. In *ACM Transactions on Graphics*, volume 22, pages 724–731, 2003.